Materials Science and Engineering C 33 (2013) 3832–3838

Contents lists available at ScienceDirect

Materials Science and Engineering C

journal homepage: www.elsevier.com/locate/msec

Microstructure, mechanical and bio-corrosion properties of Mn-doped Mg–Zn–Ca bulk metallic glass composites

Jingfeng Wang [a,*], Song Huang [a], Yang Li [a], Yiyun Wei [a], Xingfeng Xi [b], Kaiyong Cai [b]

[a] National Engineering Research Center for Magnesium Alloys, College of Materials Science and Engineering, Chongqing University, Chongqing 400044, PR China
[b] College of Bioengineering, Chongqing University, Chongqing 400044, PR China

ARTICLE INFO

Article history:
Received 6 September 2012
Received in revised form 24 April 2013
Accepted 8 May 2013
Available online 16 May 2013

Keywords:
Mg-based alloy
Amorphous
Microstructure
Mechanical properties
Biocompatibility

ABSTRACT

The effects of Mn substitution for Mg on the microstructure, mechanical properties, and corrosion behavior of $Mg_{69-x}Zn_{27}Ca_4Mn_x$ (x = 0, 0.5 and 1 at.%) alloys were investigated using X-ray diffraction, compressive tests, electrochemical treatments, and immersion tests, respectively. Microstructural observations showed that the $Mg_{69}Zn_{27}Ca_4$ alloy was mainly amorphous. The addition of Mn decreases the glass-forming ability, which results in a decreased strength from 545 MPa to 364 MPa. However, this strength is still suitable for implant application. Polarization and immersion tests in the simulated body fluid at 37 °C revealed that the Mn-doped Mg–Zn–Ca alloys have significantly higher corrosion resistance than traditional ZK60 and pure Mg alloys. Cytotoxicity test showed that cell viabilities of osteoblasts cultured with Mn-doped Mg–Zn–Ca alloys extracts were higher than that of pure Mg. $Mg_{68.5}Zn_{27}Ca_4Mn_{0.5}$ exhibits the highest bio-corrosion resistance, biocompatibility and has desirable mechanical properties, which could suggest to be used as biomedical materials in the future.

1. Introduction

Magnesium (Mg) alloys have become a topic of interest in the biomaterial field in recent years because of their potential as implant materials [1–6,13–18]. Traditional Mg alloys are bioreactive in body solutions, and their degradation rates are too high to be tolerated by human body before its functional retirement [4–6]. The bulk metallic glasses (BMGs) with single-phase, chemically homogeneous alloy system and the absence of second phases have drawn the attention of many researchers [7,8], because of its enhanced mechanical properties corrosion resistance as well as relatively more uniform corrosion properties. Of the various BMG materials, Mg–Zn–Ca BMGs are significantly more attractive because of their low density (2.0 g/cm^3) and low Young's modulus (25 GPa–45 GPa) [1,9,10], which is close to the modulus of human bones (10–40 GPa) [10]. The most important property of Mg–Zn–Ca BMGs is their ability to degrade in aqueous solutions, making them highly suitable as for biodegradable bone tissue engineering. In addition, Mg–Zn–Ca BMGs exhibit appropriate mechanical properties and consist of biological-friendly materials. These properties are important for several reasons: (1) approximately 1000 g to 1500 g Ca is present in an adult human body [11]; (2) Mg promotes Ca incorporation into the bone [4]; and (3) Zn can stimulate fracture healing in the bone, reduce postmenopausal bone loss, improve bone mineralization, and increase skeletal strength [12].

To ensure the feasibility of using Mg alloys as implants, the corrosion rates of these alloys must be reduced. Recently, Al and/or rare earth (RE) element free magnesium alloys, such as, Mg–Zn [13], Mg–Ca [14], Mg–Zn–Ca [15], Mg–Zn–Si [16], and Mg–Zn–Mn [17,18], have attracted the attention of researchers. Manganese (Mn) is an element which can be tolerated by the human body and can also retard the biodegradation of Mg alloys [19]. Also, there is no side effect if Mn was implanted into the human body [1]. It indicates that Mn is a biologically friendly element and has no toxicity that can be used for biomedical implants as well as in the improvement of corrosion behavior. Some Mn-containing Mg alloys, such as Mg–2.0Zn–0.2Mn [17], Mg–1.2Mn–1.0Zn [18], and Mg–Zn–Mn–Ca [20], have been developed and proposed for biomedical applications. Mn could also play a key role in improving the saltwater resistance of Mg alloys by removing iron and other heavy metals [21].

In this study, Mn was added to Mg–Zn–Ca BMGs. $Mg_{69-x}Zn_{27}Ca_4Mn_x$ (x = 0, 0.5, and 1 at.%) alloys were prepared to determine the effects of Mn on the phase constitution, microstructure, and mechanical properties. The in vitro degradation performance in a simulated body fluid (SBF) is also discussed in the current paper.

2. Experiment

2.1. Preparation of materials

Mixtures of Mg (99.9 wt.%), Zn (99.9 wt.%), Mg–30Ca alloy (30 wt.% Ca), and Mg–4.5Mn alloy (4.5 wt.% Mn) were melted in an induction furnace under a high-purity argon atmosphere to prepare the master alloys $Mg_{69}Zn_{27}Ca_4$ [22], $Mg_{68.5}Zn_{27}Ca_4Mn_{0.5}$, and $Mg_{68}Zn_{27}Ca_4Mn$. The master alloys were then remelted thrice by induction melting in a quartz tube to ensure that the composition was homogenous. Finally, the remelted alloys were injected into a copper mold to obtain rods

* Corresponding author. Tel.: +86 23 65112153.
E-mail address: jfwang@cqu.edu.cn (J. Wang).

0928-4931/$ – see front matter © 2013 Elsevier B.V. All rights reserved.
http://dx.doi.org/10.1016/j.msec.2013.05.020

with a diameter of 1.5 mm. The chemical compositions of the alloys were determined by chemical analysis on an X-ray fluorescence analysis (XRF), as list in Table. 1.

2.2. Microstructural and mechanical tests

The structures of the Mn-doped Mg–Zn–Ca BMGs were identified using X-ray diffraction (XRD, Rigaku D/MAX-2500PC) with Cu Kα radiation. The thermal behaviors were investigated using a differential scanning calorimeter (Perkin-Elmer DSC7) under a flowing purified argon at a heating rate of 20 K/min. Specimens with a diameter of 1.5 mm and a length of 3 mm were cut from the cast rods, and the two ends were then carefully polished to ensure parallelism. These specimens were then subjected to a compression test at a strain rate of 10^{-4} s^{-1} using a SANS CMT5105 testing machine. The microstructural morphologies and compound compositions were determined using a VegaIILMU scanning electron microscope (SEM) with an energy-dispersive X-ray spectrometer (EDS).

2.3. Electrochemical test

Electrochemical measurements were conducted in a three-electrode cell using a platinum counter electrode and a saturated calomel reference electrode. The potentiodynamic polarization curves were recorded at a potential sweep rate of 1 mV · s^{-1} at 37 °C after immersing the specimens in SBF [23–25] (8.035 g NaCl, 0.355 g $NaHCO_3$, 0.225 g KCl, 0.231 g $K_2HPO_4 \cdot 3H_2O$, 0.311 g $MgCl_2 \cdot 6H_2O$, 0.292 g $CaCl_2$, 0.072 g Na_2SO_4, and 6.118 g $(HOCH_2)_3CNH_2$) for 30 min and when the open-circuit potential (OCP) became nearly constant.

2.4. Immersion test

For the immersion test, cylindrical samples with Φ1.5 mm × 10 mm were cut from the copper mold injected samples and the as-cast pure Mg sample. The immersion test was performed in 10 ml SBF solutions, with the temperature kept at 37 °C using a water bath. Before the immersion, the pH of SBF solution was adjusted to 7.3. The SBF solution was changed every three days. At the first 3 days of the immersion, we examined the change of the pH values of each experimental solution. After different immersion times, the samples were removed from the SBF solution, gently rinsed with distilled water, and then dried at room temperature. A VegaIILMU SEM was used to observe the surface morphologies. The average of three measurements (the hydrogen evolution and the change of the pH values) was taken for each sample.

2.5. Cytotoxicity test

The cytotoxicity test was carried out by the indirect contact. Osteoblasts were harvested from neonatal rat calvaria with a sequential collagenase digestion method. They were cultured in Dulbecco's modified Eagle's medium (DMEM), 10% fetal bovine serum (FBS), 100 U/ml penicillin and 100 mg/ml streptomycin at 37 °C in a humidified atmosphere of 5% CO_2. Osteoblasts at the 3rd passage were used in the following experiments.

Table 1
Chemical composition of Mg–Zn–Ca–Mn alloys.

Samples	Chemical composition							
	Mg		Zn		Ca		Mn	
	wt.%	at.%	wt.%	at.%	wt.%	at.%	wt.%	at.%
$Mg_{69}Zn_{27}Ca_4$	47.08	69.44	48.46	26.57	4.46	3.99	–	–
$Mg_{68.5}Zn_{27}Ca_4Mn_{0.5}$	45.13	67.74	49.68	27.72	4.53	4.13	0.66	0.41
$Mg_{68}Zn_{27}Ca_4Mn$	45.58	68.42	48.36	26.98	4.08	3.72	1.38	0.88

The extracts of the samples were prepared by the DMEM serum free medium, with the surface area/extraction medium ratio 1 cm^2/ml in a humidified atmosphere with 5% CO_2 at 37 °C. After 72 h incubation, the supernatant fluid was withdrawn and centrifuged to prepare the extraction medium. Then the extraction medium was serially diluted to 10% concentration. The extraction medium was refrigerated at 4 °C before the cytotoxicity test. The control groups involved the use of DMEM medium as negative control in this experiment.

Cells were incubated in 96-well cell culture plates at an initial density of 5 × 10^3 cells/well with 100 μl DMEM medium and incubated for 24 h to allow attachment. Then the medium was replaced with 100 μl of extracts. After incubating the cells in a humidified atmosphere with 5% CO_2 at 37 °C for 3 days, 10 μl cell counting kit (CCK-8) was added and then the samples were incubated with CCK-8 in DMEM in at 37 °C for 4 h. The spectrophotometrical absorbance of the samples was measured by microplate reader (Bio-RAD 680) at 570 nm.

3. Results

3.1. Microstructure

Fig. 1 shows the XRD patterns of the $Mg_{69}Zn_{27}Ca_4$, $Mg_{68.5}Zn_{27}Ca_4Mn_{0.5}$, and $Mg_{68}Zn_{27}Ca_4Mn$ alloy rods. The results show that $Mg_{69}Zn_{27}Ca_4$ was fully amorphized except for a typical broad halo diffraction peak, which confirms the absence of a crystalline phase despite the sensitivity of the XRD technique. However, for $Mg_{68.5}Zn_{27}Ca_4Mn_{0.5}$, some crystalline peaks appeared on the broad diffraction hump, which indicates the coexistence of crystalline and amorphous phases. Furthermore, the broad peaks gradually disappeared as Mn increased, as observed in the $Mg_{68}Zn_{27}Ca_4Mn$ alloy. Therefore, the XRD results show that Mn microalloying can disrupt the glass forming ability (GFA).

Fig. 2 displays the DSC curves of the three alloys above mentioned. The glass transition and crystallization behaviors of these alloys are shown in Fig. 2a. The $Mg_{69}Zn_{27}Ca_4$ alloy rod underwent a clear glass transition endothermic and exothermic crystallization and thus exhibits an amorphous structure. However, the thermal behavior of this alloy significantly changed even if a scantling Mn doped, as indicated by the glass transition temperature Tg disappeared, the onset crystallization temperature Tx raised dramatically and the heat of crystallization ΔH rapidly diminished for the $Mg_{68.5}Zn_{27}Ca_4Mn_{0.5}$ alloy, which shows that the GFA become poor [26] with the addition of Mn. In addition, all of the Mg–Zn–Ca–Mn alloys show two melting peaks in the high temperature melting stage (Fig. 2b). The thermal parameters, including Tx, ΔH_x, Tm, and the liquid temperature Tl, of the three alloys are summarized in Table 2.

The three alloys were further examined using SEM-EDS to illustrate the effect of partial substitution of Mg by Mn on the structural evolution. The SEM backscattered electron images (Fig. 3) show the differences

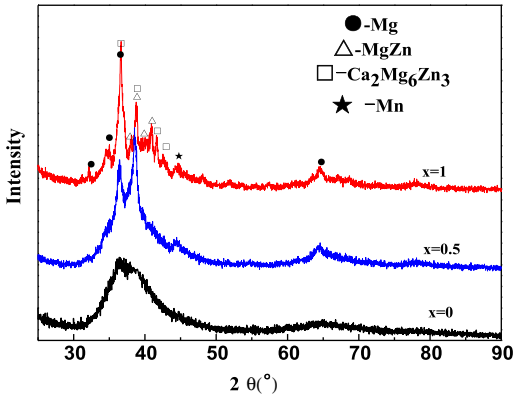

Fig. 1. X-ray diffraction (XRD) patterns of the as-cast $Mg_{69-x}Zn_{27}Ca_4Mn_x$ (x = 0, 0.5, and 1 at.%) alloys.